IPP-Report

IPP Max-Planck-Institut für Plasmaphysik

P.T. Lang, J. Neuhauser, K. Büchl,
M. Kaufmann, R.S. Lang, A. Lorenz,
V. Mertens, H.W. Müller, H. Salzmann
and ASDEX Upgrade Team

Controlled High Density Operation on ASDEX Upgrade by Pellet Refueling from the Magnetic High-Field Side

IPP 1/314
February 1998

CONTROLLED HIGH DENSITY OPERATION ON ASDEX UPGRADE BY PELLET REFUELING FROM THE MAGNETIC HIGH-FIELD SIDE

P.T. Lang, J. Neuhauser, K. Büchl, M. Kaufmann, R.S. Lang, A. Lorenz, V. Mertens, H.W. Müller, H. Salzmann, ASDEX Upgrade Team

Max-Planck-Institut für Plasmaphysik
EURATOM Association
Boltzmannstr. 2, 85748 Garching, Germany

ABSTRACT

A novel, highly efficient tokamak plasma refueling scenario with cryogenic deuterium (D) pellets injected from the magnetic high-field side was applied for the first time to demonstrate feedback-controlled operation beyond the empirical Greenwald density limit. In this scheme, a centrifuge injector was used to inject pellets via a funnel and a guiding tube at velocities of 240 m/s and repetition rates up to 30 Hz. The pellet particle fluxes achieved were capable to achieve stable operation at about 1.2 times the Greenwald limit with a supporting gas puff of about the same amount. In contrast to low-field side pellet injection, no significant pellet induced confinement degradation and density profile peaking were observed. The H-mode was maintained during high density operation with an energy confinement time normalized to the ELMy H-mode 0.85 * ITERH93P scaling of above 0.82. The density gradient at the plasma edge already achieved during the pre-pellet H-mode phase shows no significant increase during the pellet induced increase of plasma inventory. The particle flux through the edge is about 5 times higher during the pellet phase than before. This seems to indicate a strong increase of the particle diffusivity at the plasma edge enforced by the pellet particle source.

Table of Contents

1. INTRODUCTION

In order to achieve thermonuclear burn, future fusion experiments must safely operate at rather high density, while retaining at the same time sufficiently high energy confinement [1]. Present experiments show, however, that useful tokamak operation space is limited towards high density by various processes such as excessive edge radiation cooling eventually causing a disruption, the onset of fast MHD-instabilities (e.g. ballooning limit), or simply untolerable energy confinement degradation (e.g. loss of H-mode).

Despite the obvious role of the edge energy balance in most disruptive discharges, an early multi-machine study for gas puffed L-mode plasmas indicated an ultimate, essentially power independent limit for the line averaged density in well-conditioned discharges [2]. A simple formulation was derived for this empirical "Greenwald limit"

$$\overline{n_{e,Gw}}\left[10^{20}\ m^{-3}\right] = \frac{I_P[MA]}{\pi\ a_0^2[m^2]}$$

depending on the plasma current I_P and the minor radius a_0 only, in contrast to expectations based on edge radiation and power balance models. A severe particle confinement degradation when approaching this limit was suggested as an explanation.

Meanwhile, line averaged densities beyond this limit have been reported from several limiter and divertor tokamaks with gas puffing. In all cases peaked density profiles were observed, indicating a limitation of the edge density rather than that of the line averaged density. Though originally derived for L-mode plasmas, this empirical scaling formula also seems to describe the upper density limit observed with gas puffing in H-mode, i.e. the density above which the the plasma falls back into L-mode [3]. This means that both, particle and energy confinement might be degrading severely as soon as a critical (edge) density of the order of the Greenwald density is exceeded.

Energy confinement scaling in tokamaks has been intensely studied, especially as part of the ITER R&D effort, and various scaling formulas have been derived on a statistical basis [4], e.g. ITER89P for L-mode, ITER92 for ELMy H-mode or ITERH93P for the ELM-free H-mode. The

scalings do not represent such a strict limit, probably since the overwhelming part of the experimental data base refers to densities well below the limit. Obviously, much more data are needed at the high density end, and the simultaneous achievement of high density with high energy confinement time remains a major challenge. The development of such high density, high performance scenarios was and still is a key element of the ASDEX Upgrade programme [5].

Experimentally, the most direct method to achieve line averaged densities beyond Greenwald is the injection of cryogenic hydrogen pellets. This way stationary H-mode operation was demonstrated, albeit with reduced H-mode quality. A disadvantage of the standard pellet injection scheme relying on pellet launch from the (easily accessible) torus outside is that with increasing heating power the fueling efficiency drops significantly [6,7], accompanied by an additional pellet induced confinement drop. Fortunately, this deficiency can be removed to a large extent by high field side injection as shown recently on ASDEX Upgrade [8].

A major task of pellet injection experiments performed at ASDEX Upgrade was to verify and improve the feasibility of the pellet option for ITER. In this paper we report on recent progress with respect to feedback controlled, quasi-stationary plasma operation beyond the Greenwald limit with continuous pellet injection using different launching geometries. "Best" results of the injection from the low-field side are reviewed and compared with preliminary results obtained with centrifuge driven pellet injection from the high-field side. The latter demonstrate the future potential of this new scheme. The influence of the particle source distribution on the edge particle transport in high density plasmas is discussed.

In order to provide some idea of the discharge quality achieved, we use throughout this paper the Greenwald formula [2] and the 0.85* ITER93 ELM-free scaling [4] for density and confinement normalization, respectively, despite the lack of a generally accepted physical model behind these empirical scalings.

2. WHY HIGH FIELD SIDE INJECTION?

One of the major programme points on the ASDEX Upgrade poloidal divertor tokamak is to establish safe high density, high power operation scenarios feasible for future fusion experiments. Cryogenic pellet fueling, implemented already at old ASDEX [9], is a key element of this programme. As a first step on ASDEX Upgrade, a newly developed centrifuge pellet injector was employed for repetitive injection at rates up to 80 Hz using the usual injection scheme from the torus outside, i.e. the magnetic low field side (LFS). In this mode of pellet injection the same problems as in other tokamak facilities were encountered. The major problem was fast radial particle transport on a timescale less than 100 μs, resulting in a degradation of the fueling efficiency (ratio of pellet induced plasma particle inventory / pellet particle inventory) with increasing heating power. This behaviour is attributed to the transient formation of a high β pellet ablation cloud (plasmoid) on a time scale of a few tens of μs. We conclude that the rapid increase of the local kinetic plasma pressure causes a curvature driven radial acceleration [10-12], resulting in a strong radial shift of the ablated and ionized particles towards the magnetic low field side. If the average displacement is larger than the penetration depth, as expected for sufficiently hot plasmas, then part of the deposited material may be lost immediately as observed in experiment (additional losses on a somewhat slower time scale, not discussed here in detail, are expected and observed for shallow deposition in ELMy H-mode discharges because of ELM triggering [7]). The fast particle losses were accompanied by a corresponding, pellet induced energy confinement degradation. Nevertheless, feedback controlled stationary operation at a density level up to 1.5 times the Greenwald limit was successfully demonstrated with LFS injection on ASDEX Upgrade, albeit at the expense of degraded confinement and low fueling efficiency.

Injection from the magnetic high field side (HFS) was tried for the first time at ASDEX Upgrade [8], to overcome these fast losses in hot target plasmas. In this scheme the plasmoid acceleration, directed towards the plasma center, was expected to inhibit particle losses and even allow deeper penetration and fueling. In order to understand this question, a preliminary setup was installed at ASDEX Upgrade: pellets from a blower gun were launched into the same discharge

from the LFS as well as from the HFS via guiding tubes. Despite the rather limited velocity and repetition rate of this setup, HFS injection proved to be clearly superior to LFS injection. During HFS injection, fueling efficiencies were high and showed no degradation with increasing heating power up to the highest power applied. Moreover, deeper penetration of the frozen pellet was observed for HFS injection with respect to LFS pellets. This was attributed to precooling in front of the slowly travelling pellet resulting from the high β plasmoid moving ahead of the pellet. However, the low repetition rate did not allow for strong density build up, although densities near the Greenwald limit were transiently obtained after each pellet. In the next step, pellets were accelerated by the centrifuge injector (the same as used for LFS injection), but guided to the high field side of the plasma through a bent tube in a similar fashion as with the blower gun. First successful results obtained with this improved arrangement are reported below.

3. EXPERIMENTAL ARRANGEMENT AND DIAGNOSTICS

ASDEX Upgrade [13] is a midsize divertor tokamak (major radius R = 1.65 m, minor radius a_0 = 0.5 m, typical elongation k = 1.6), usually operated with a single-null divertor configuration. All plasma facing components are graphite and the vessel is routinely boronised. Four beamlines of the first NI injector, able to produce a 'staircase' power waveform up to 10 MW, are applied for plasma heating in addition to ohmic heating. Several calibrated valves mounted at the vessel midplane are used for gas puffing and turbomolecular pumps with a pumping speed of 14 m^3/s for D control the particle exhaust. The cryopump was not yet in operation during the experiments described here.

Until 1996, the more open DV-I divertor configuration was used, since spring 1997 the more closed new Lyra (DV-II) divertor configuration [14] is in operation. All pellet experiments until the first demonstration of HFS refueling (#8506) were performed with the DV-I divertor configuration, the experiments of HFS pellet injection (from #8943) using the centrifuge were performed with the DV-II configuration. The change of the setup is shown in figure 1.

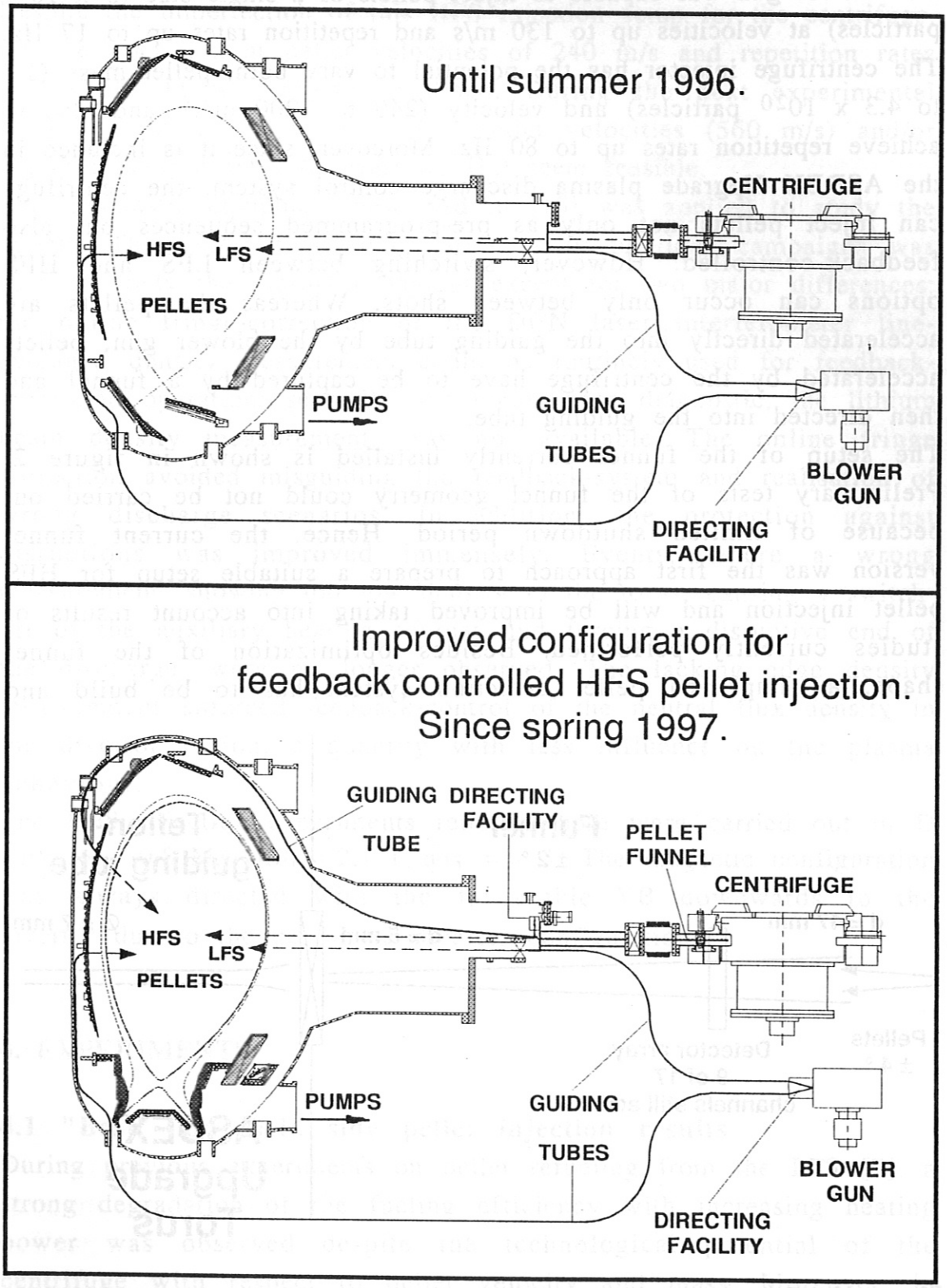

Figure 1: Changed experimental setup during the 1996/97 shutdown. During this shutdown the DV-I configuration was replaced by the new Lyra (DV-II) configuration; the centrifuge injector was enabled to inject pellets via guiding tubes from the magnetic high field side.

The blower gun was capable to inject pellets of a single size (3 x 10^{20} particles) at velocities up to 130 m/s and repetition rates up to 17 Hz. The centrifuge injector has the potential to vary both, pellet mass (1.7 to 4.3 x 10^{20} particles) and velocity (240 to 1200 m/s), and also to achieve repetition rates up to 80 Hz. Moreover, since it is included in the ASDEX Upgrade plasma discharge control system, the centrifuge can inject pellets not only as pre-programmed sequences but also feedback-controlled. However, switching between LFS and HFS options can occur only between shots. Whereas the pellets are accelerated directly into the guiding tube by the blower gun, pellets accelerated by the centrifuge have to be captured by a funnel and then directed into the guiding tube.

The setup of the funnel currently installed is shown in figure 2. Preliminary tests of the funnel geometry could not be carried out because of limited shutdown period. Hence, the current funnel version was the first approach to prepare a suitable setup for HFS pellet injection and will be improved taking into account results of studies currently performed. Besides optimization of the funnel shape, an improved pellet detection system has to be build and

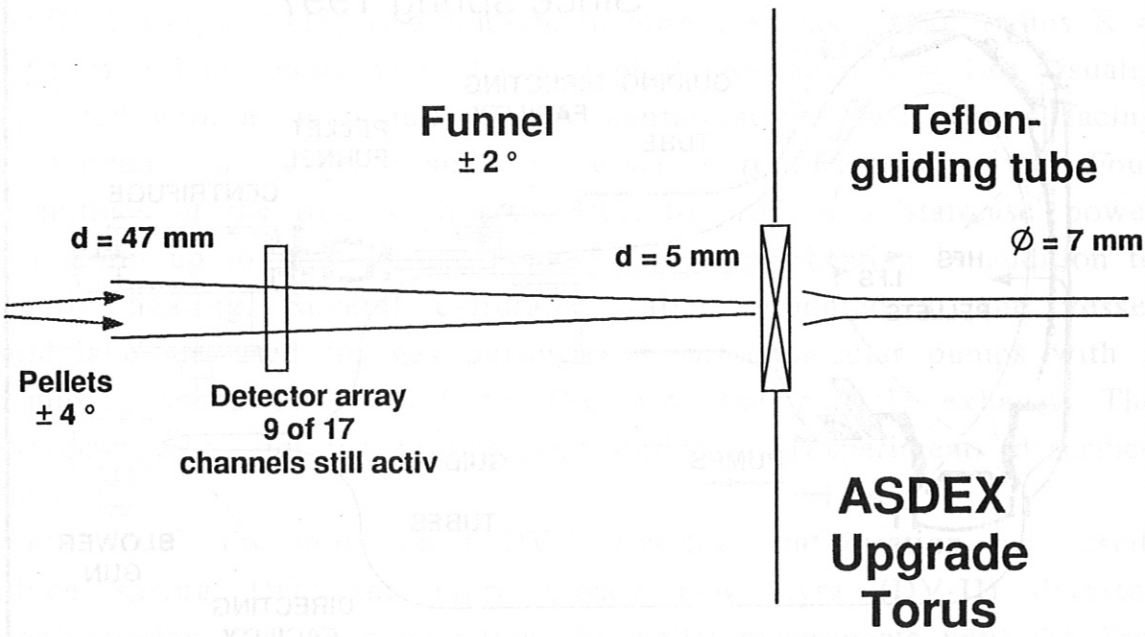

Figure 2: Schematic of the funnel installed at the centrifuge exit to capture pellets and direct them into the guiding tube. The surface of the first funnel version is covered by Viton®. The detector array installed for adjustment of the pellet exit direction is partially shaded by the funnel.

installed, since the available layout was optimized for LFS injection. Despite the imperfection of this HFS injection setup for the centrifuge, reliable operation at pellet velocities of 240 m/s and repetition rates up to 30 Hz was already realised. During the next experimental campaign improvements to higher pellet velocities (560 m/s) and/or higher repetition rates (at least 60 Hz) seem feasible.
The diagnostic equipment described in [15] was applied to study the pellets. The same set of diagnostics as in previous campaigns was used to study the plasma behaviour except for two major differences: the online fringe-correction of the DCN laser interferometer line-averaged density measurement could be routinely used for feedback-controlled operation; secondly one major edge diagnostic, the lithium beam density measurement, was not available. The online fringe correction avoided misguiding the feedback-system and realisation of wrong discharge scenarios. In addition, the protection against disruptions was improved immensely. Events, where a wrong measurement, showing too low density in the torus, causing a switch-off of the auxiliary heating sources and forcing a disruptive end of the discharge, were no longer observed. The lacking edge density measurement enforced feedback-control of the neutral flux density in the divertor region, a quantity with less influence on the plasma behaviour.
The HFS injection experiments reported here were carried out in D with I_P = 0.8 MA, $|B_t|$ = 2.1 T, q_{95} = 4.3. The magnetic configuration was always directed with the favourable ∇B downwards to the divertor due to the new Lyra divertor configuration.

4. EXPERIMENTS

4.1 "Best" low field side pellet injection results

During previous experiments on pellet refueling from the LFS [7], a strong degradation of the fueling efficiency with increasing heating power was observed despite the technological potential of the centrifuge with respect to pellet velocity and mass. Moreover, in ELMy H-mode discharges a further degradation was observed for shallow penetration at low pellet velocities. This behaviour is thought to be caused by a pellet particle deposition profile effectively shifted towards the plasma edge with respect to the ablation profile by the

toroidal curvature drift [10-12]. A massive loss of particles is then induced by an ELM triggered by the pellet itself.
Maximum efficiency realized in this scenario is represented by a solid line in figure 3. However, as can be seen, even a nil response was observed for high heating powers under unfavourable conditions. No significant power degradation of the fueling efficiency was observed for HFS pellet injection despite limited pellet velocities for pellets injected by both, blower gun and centrifuge. The scatter of observed ε_f values is most probably caused by pellet mass losses during transfer to the plasma, as for calculating ε_f nominal pellet masses at the injector exit were used. From the data shown in figure 3 it can also be concluded that a doubled pellet velocity - realized by pellets injected with the centrifuge instead of the blower gun - shows no noticeable further enhancement in efficiency. This matches rather well with the assumption of a cooling wave travelling ahead of the pellet, making the pellet velocity a rather unimportant parameter (as long as it is much slower than the velocity of the plasmoid).
The fast particle losses following the LFS pellet injection, which were getting stronger with increasing plasma temperature and/or when entering the H-mode, were accompanied by further unfavourable changes in the plasma performance. First of all, an increased repetition rate and therefore pellet particle flux had to be applied in order to counterbalance the losses. This caused in some cases nonstationary refueling: pellets caused persistent plasma cooling, and increasing pellet penetration resulted in central deposition. Although very high line-averaged densities could be achieved this way due to the strong peaking of the density profile, this effect is only of little use as it is of transient nature. Therefore it seems not scale towards a fusion reactor because central pellet deposition under appropriate plasma conditions is almost impossible for technical reasons.
In some cases, the high pellet particle flux caused persistent profile peaking even for stable deposition. This might be a consequence of the application of a repetition rate too high, changing the transport inside the core plasma. Such behaviour has been observed in earlier experiments on ASDEX Upgrade with pellet injection [15], where density profile peaking occured only above a certain repetition rate. An example is shown in figure 4, where the temporal evolution of the most important plasma parameters is shown for a discharge with LFS pellet injection at a pellet rate of 76 Hz. This discharge was

performed to demonstrate feedback controlled operation at densities beyond the Greenwald limit and represented the optimum performance obtained for the LFS scenario so far.

A moderate but persistent peaking of the density profile - represented by the value $n_{e0}/\overline{n_e}$ - still remains after the density buildup is already finished. Such a behaviour might cause problems for longer durations due to e.g. central impurity accumulation [9].

Another major problem resulting from strong pellet particle losses is the degradation of the energy confinement. This can be seen clearly in figure 4, where both, plasma energy and energy confinement time show strong degradation correlated to pellet injection (indicated by the spikes in the D_α radiation and the pellet request signal).

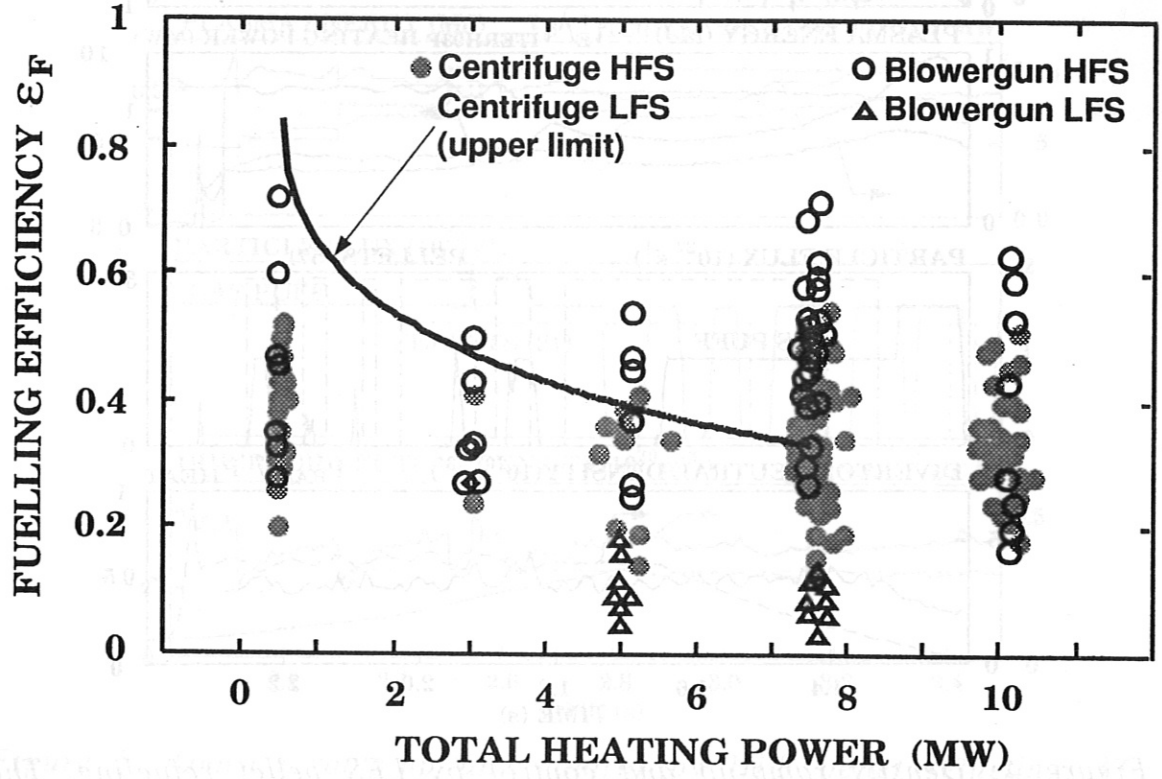

Figure 3: Fueling efficiency calculated on the assumption of a nominal pellet mass versus total heating power. The degradation observed for LFS pellet injection (solid line representing limiting curve of maximum values obtained for ideal conditions) is not observed for HFS injection with the centrifuge (filled symbols) or the blower gun (open symbols). The nominal pellet mass was determined at the injector exit in laboratory experiments.

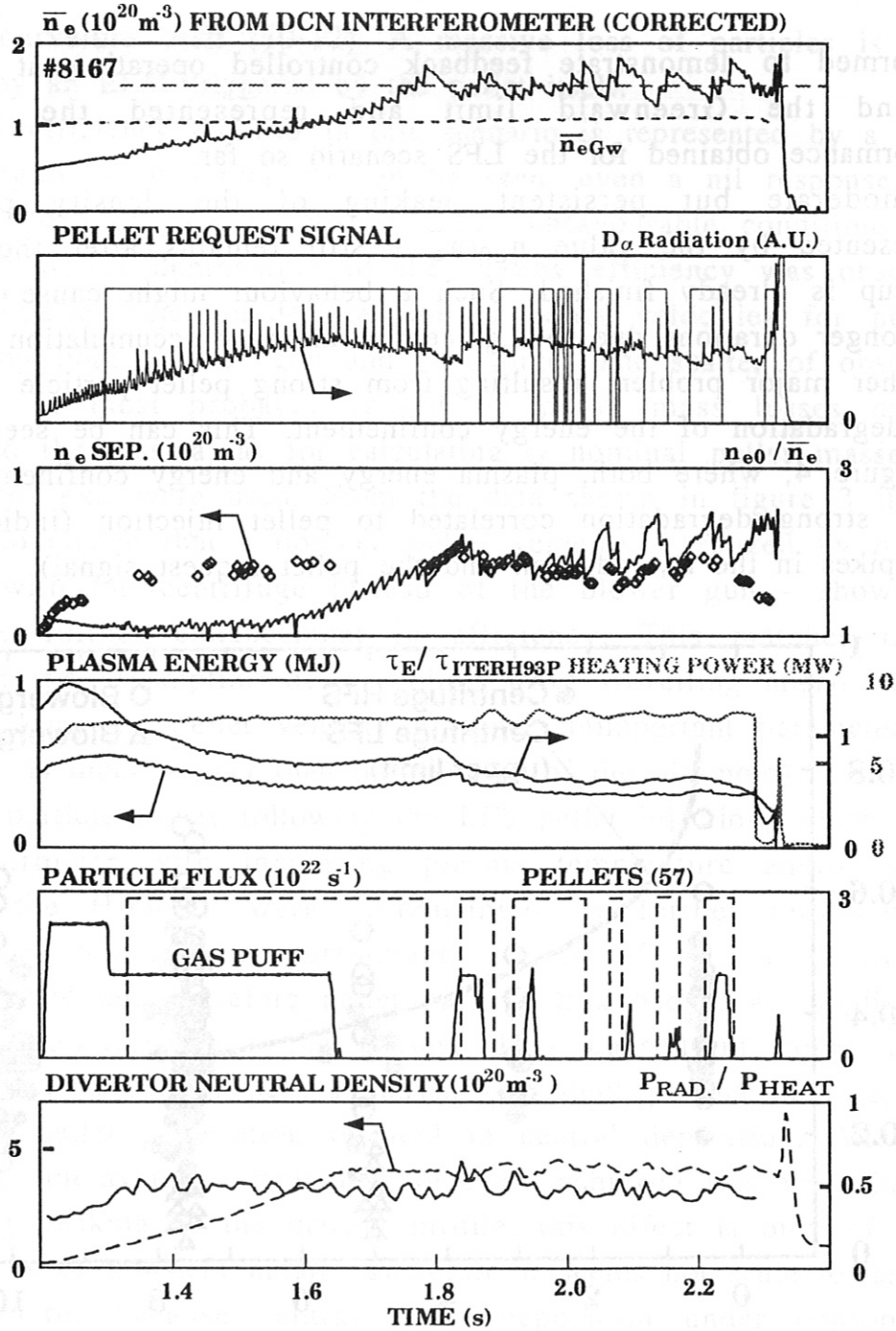

Figure 4: Density ramp-up and control by LFS pellet refueling. The line-averaged density (upper trace) is adjusted to an envisaged value of 1.5 x 10^{20} m^{-3} by pellet injection (indicated by the spikes in the D_α signal). The pellet particle flux applied was sufficient to enable the requested density build-up almost without supporting gas puffing. However, degradation of plasma energy and energy confinement occurs during the pellet sequences. Moreover, the density profile keeps peaking even once the density had reached the requested level. The disruptive end was caused by fringe losses of the interferometer.

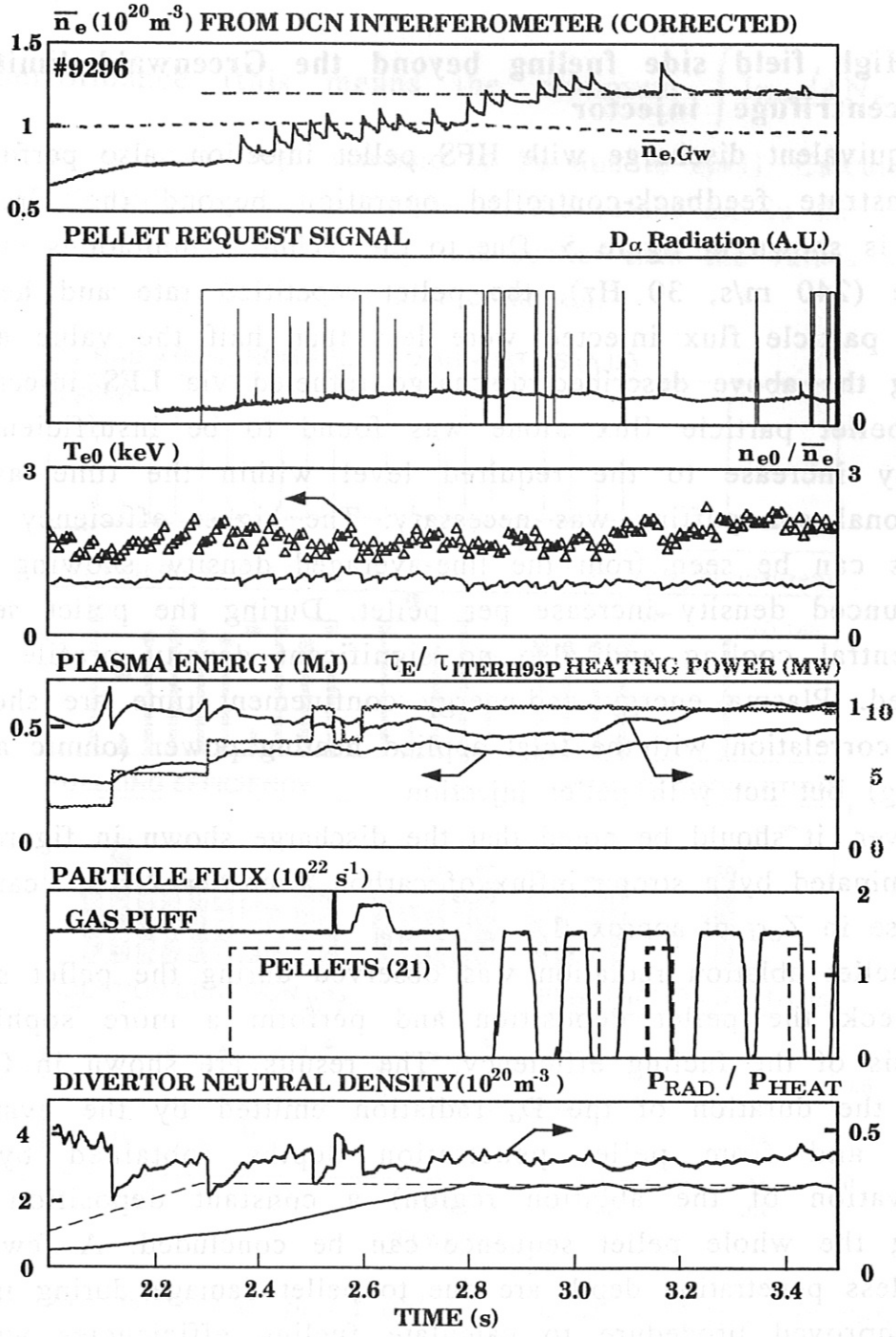

Figure 5: Density ramp-up and control by HFS pellet refueling. The line-averaged density (upper trace) is adjusted to an envisaged value of 1.2 x 10^{20} m^{-3} by pellet injection (indicated by the spikes in the D_α signal). The pellet particle flux had to be supported by gas puffing in order to enable the requested density build-up within time. No significant degradation of plasma energy and energy confinement occurs during the pellet sequences; also no significant density profile peaking is observed.

4.2 High field side fueling beyond the Greenwald limit using the centrifuge injector

An equivalent discharge with HFS pellet injection, also performed to demonstrate feedback-controlled operation beyond the Greenwald-limit, is shown in figure 5. Due to the technical limitations mentioned before (240 m/s, 30 Hz), the pellet repetition rate and hence the pellet particle flux injected were less than half the value available during the above described discharge refueled via LFS injection. As this pellet particle flux alone was found to be insufficient for a density increase to the required level within the time available, additional gas puffing was necessary. The higher efficiency of HFS pellets can be seen from the line-averaged density, showing a more pronounced density increase per pellet. During the pellet sequence, no central cooling and also no significant density profile peaking occured. Plasma energy and energy confinement time are showing a clear correlation with the total applied heating power (ohmic and NBI heating) but not with pellet injection.

However, it should be noted that the discharge shown in figure 5 was contaminated by a strong influx of carbon after t = 2.7 s, causing an increase in Z_{eff} of approx. 1.

The pellet ablation radiation was observed during the pellet sequence to check the pellet deposition and perform a more sophisticated analysis of the fueling efficiency. The results are shown in figure 6. From the duration of the D_α radiation emitted by the evaporating pellet and from pellet penetration depths (obtained by video observation of the ablation region) a constant deposition profile during the whole pellet sequence can be concluded. A few pellets with less penetration depth are due to pellet damage during injection. An improved procedure to calculate fueling efficiencies was tried making use of the recorded ablation radiation signals. The total amount of ablation radiation $\int I_{D\alpha}$ was calculated using a fit procedure to suppress the background radiation for each single pellet. The obtained values correlate rather well with the pellet induced plasma particle increase (rms deviation 0.146 for the complete sequence), so that a calibration of these values to the injected pellet mass was performed. Ohmic discharges were calibrated under the assumption that the observed increase in pellet induced plasma inventory, ΔN_e, corresponds to the pellet mass for the pellet with the

best performance (this means the minimum $\int I_{D\alpha} / \Delta N_e$ value obtained in all shots was assumed to be due to ε_f=1). Calculating ε_f this way (shaded columns in figure 6), the values are in the order of 0.6 to 0.8 and show significantly less scatter than the values obtained assuming a fixed pellet mass (solid columns).

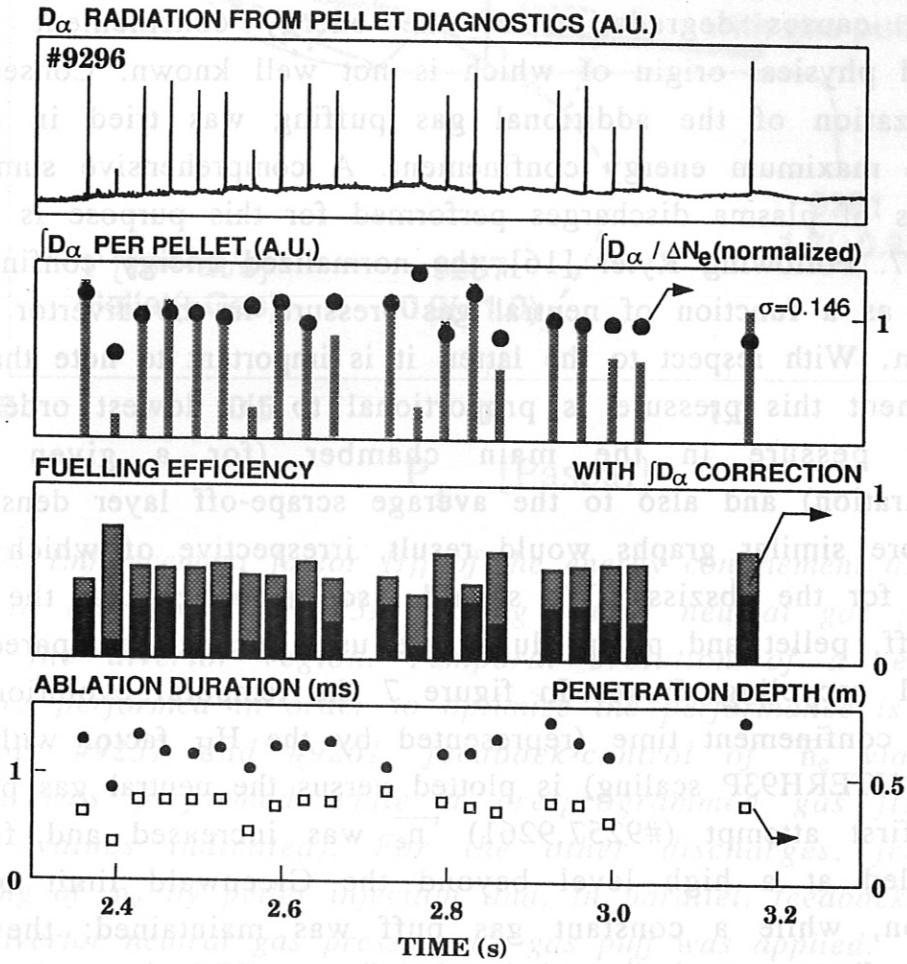

Figure 6: The amount of pellet ablation radiation ($\int I_{D\alpha}$) is correlated with the pellet induced plasma particle inventory increment (ΔN_e). Taking this value as a measure of the injected pellet mass, much higher fueling efficiencies (shaded columns) and less scatter is obtained than for the simple assumption of a fixed pellet mass and negligible pellet transfer losses (solid columns). During the whole sequence, ablation duration and pellet penetration depth stay constant (the few examples with significantly reduced values correspond to small $\int I_{D\alpha}$ values and are therefore most probably due to pellets damaged during injection).

4.3 The effect of pellets vs. residual gas puff flux on confinement

As already mentioned, HFS pellet injection was not yet sufficient to realize the required density increase (to $\overline{n_e}$ =1.2 x 10^{20} m^{-3}, approx. 1.2 × $\overline{n_{e,Gw}}$ for the plasma configuration used) within the available time, making additional gas puffing necessary. However, strong gas puffing causes degradation of the energy confinement [3], the detailed physical origin of which is not well known. Consequentely, minimization of the additional gas puffing was tried in order to achieve maximum energy confinement. A comprehensive summary of a series of plasma discharges performed for this purpose is given in figure 7. Following Ryter [16], the normalized energy confinement is plotted as a function of neutral gas pressure in the divertor pumping plenum. With respect to the latter, it is important to note that in the experiment this pressure is proportional to the lowest order to the neutral pessure in the main chamber (for a given divertor configuration) and also to the average scrape-off layer density [17]. Therefore similar graphs would result, irrespective of which one we choose for the abszissa. We should also emphasize that the external gas puff, pellet and pump fluxes are usually small compared to the internal recycling fluxes. In figure 7 the temporal evolution of the energy confinement time (represented by the H_H factor with respect to 0.85*ITERH93P scaling) is plotted versus the neutral gas pressure.
In a first attempt (#9257,9261) $\overline{n_e}$ was increased and feedback-controlled at a high level beyond the Greenwald limit by pellet injection, while a constant gas puff was maintained; the applied particle fluxes are indicated in the figure. With increasing plasma density and recycling fluxes, the energy confinement is gradually degrading as with gas puff only. Beyond a certain, discharge-dependent neutral pressure, however, the confinement drops dramatically.
In an alternative approach, the divertor neutral pressure was raised and then kept constant by feed-back controlling the external gas puff. In a second, independent control loop the line density was controlled at a high level beyond the Greenwald limit by interrupting the pellet train as required. Trajectories obtained for a requested n_{0Div} level of 2 x 10^{20} m^{-3} (#9293), 2.5 x 10^{20} m^{-3} (#9296), and 3 x 10^{20} m^{-3} (#9295) are given. At too low gas puff rates the requested density

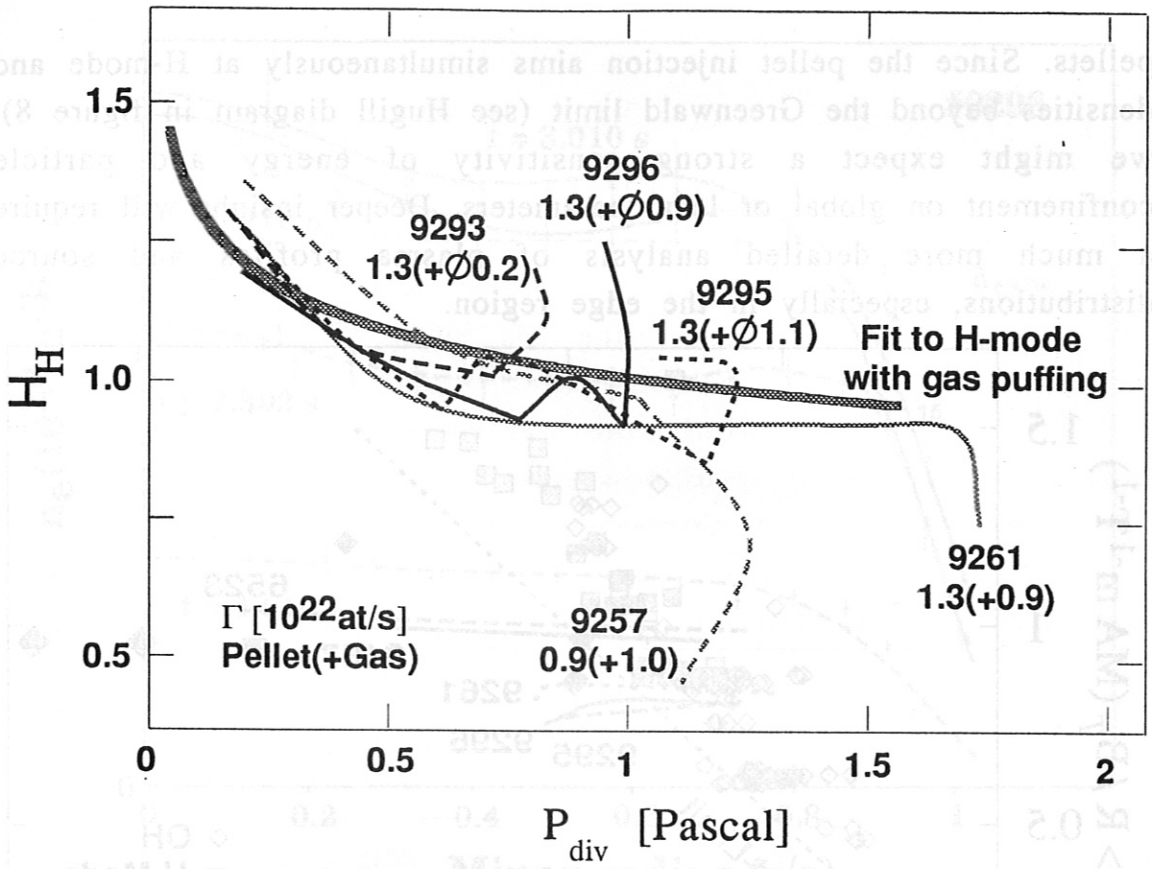

*Figure 7: Enhancement factor H_H of the energy confinement time with respect to the 0.85*ITERH93P scaling versus neutral gas pressure P_{Div} in the divertor region. Temporal evolution of a series of discharges performed in order to optimize the performance is shown. For shots #9257 and #9261, feedback-control of $\overline{n_e}$ via pellet injection was performed while a pre-programmed gas flux was applied (values indicated). For the other discharges, feedback-controlling of $\overline{n_e}$ by pellet injection and, in parallel, feedback-control of the divertor neutral gas pressure by gas puff was applied.*

level could not be reached. In #9293, where the best performance with respect to confinement degradation was obtained, $\overline{n_e}$ stayed at approx. 1.0 x 10^{20} m^{-3}, about the Greenwald limit. Again, the energy confinement is gradually degrading with increasing neutral pressure, but increases now beyond a certain discharge-dependent neutral pressure, in parallel to a reduction of the required pellet flux. Obviously, the simple relation between confinement and neutral pressure does not hold for pellet fueled discharges indicating that there are other important parameters. It is likely that the particle source distribution plays a key role in this context because of the strongly different penetration depths of neutral gas and frozen

pellets. Since the pellet injection aims simultaneously at H-mode and densities beyond the Greenwald limit (see Hugill diagram in figure 8), we might expect a strong sensitivity of energy and particle confinement on global or local parameters. Deeper insight will require a much more detailed analysis of plasma profiles and source distributions, especially in the edge region.

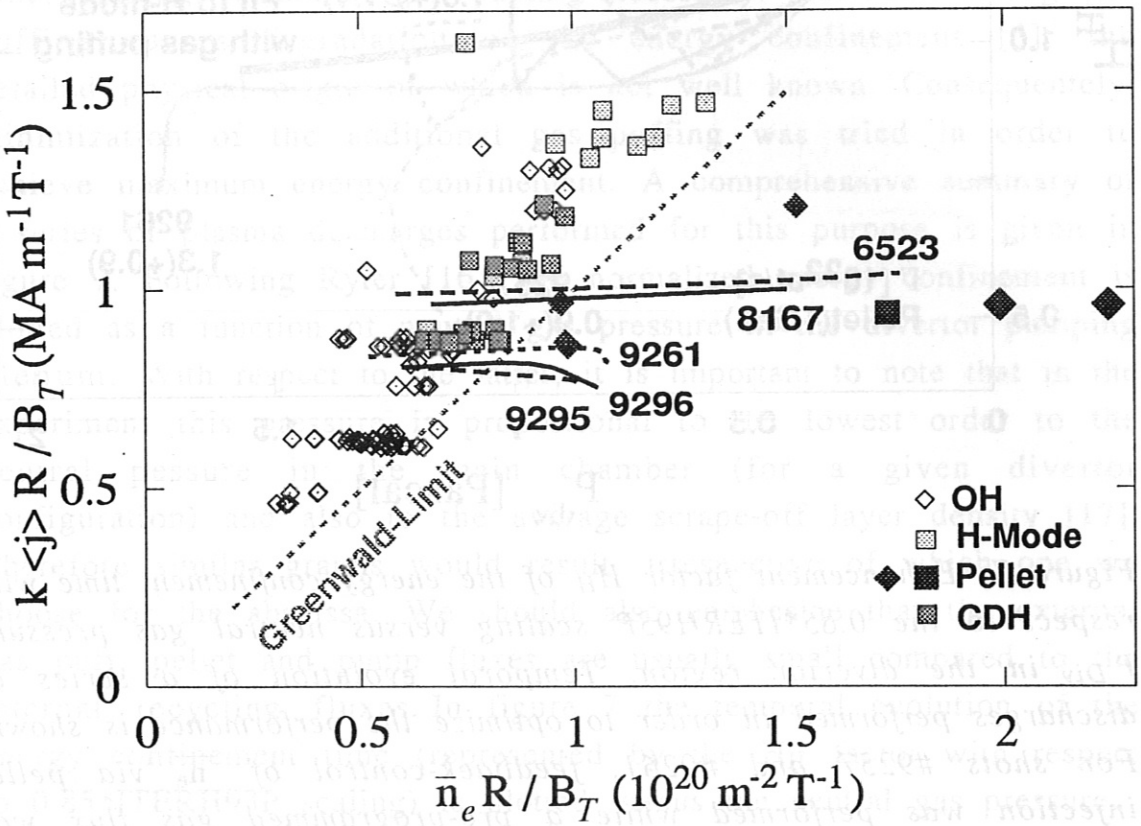

Figure 8: Hugil diagram representing the operational area of ASDEX Upgrade. Whereas discharges without pellet injection are limited approximately to the Greenwald limit, pellets give access also to the region beyond.

4.4 Particle sources and transport

In a first attempt, we analyse qualitatively the variation in density profile and particle transport before and during pellet injection in the phase where the particle inventory increases and $\overline{n_e}$ reaches values beyond the Greenwald density with pellet injection. Density profiles measured by Thomson scattering in #9296 at 4 different times are given in figure 9. Also plotted is the time evolution of the line averaged density and the density gradient, ∇n, in the plasma edge region, derived from local measurements of two adjacent Thomson channels in the plasma boundary region by

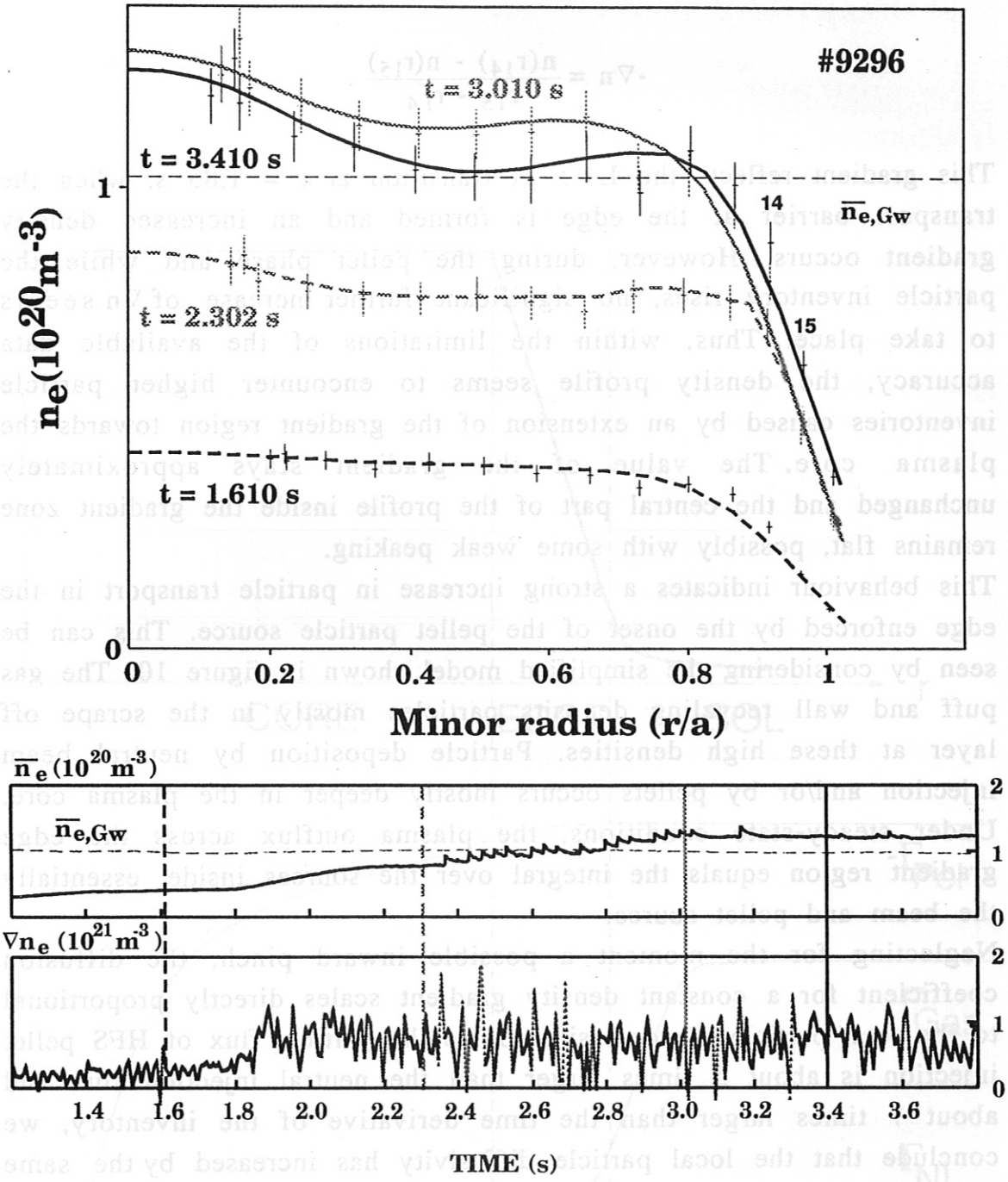

Figure 9: Evolution of the density profile as measured by Thomson scattering during #9296. Corresponding times of the 4 profiles are indicated in the time traces. The gradient in the plasma edge was calculated from the difference of the two adjacent channels 14 and 15 (distance approx. 20 mm). The transition from the L-mode (dashed black) to the pre-pellet H-mode (dashed grey) profile is indicated by an increasing gradient at the edge. During the pellet phase, both, during the density ramp up (solid black) and control phase (solid grey), the gradient in the edge seems to remain unchanged but the gradient zone extends towards the plasma core.

$$-\nabla n = \frac{n(r_{14}) - n(r_{15})}{r_{15} - r_{14}} .$$

This gradient reflects the L -> H transition at t = 1.85 s, when the transport barrier at the edge is formed and an increased density gradient occurs. However, during the pellet phase and while the particle inventory rises, no significant further increase of ∇n seems to take place. Thus, within the limitations of the available data accuracy, the density profile seems to encounter higher particle inventories caused by an extension of the gradient region towards the plasma core. The value of the gradient stays approximately unchanged and the central part of the profile inside the gradient zone remains flat, possibly with some weak peaking.

This behaviour indicates a strong increase in particle transport in the edge enforced by the onset of the pellet particle source. This can be seen by considering the simplified model shown in figure 10. The gas puff and wall recycling deposits particles mostly in the scrape off layer at these high densities. Particle deposition by neutral beam injection and/or by pellets occurs mostly deeper in the plasma core. Under steady-state conditions, the plasma outflux across the edge gradient region equals the integral over the sources inside, essentially the beam and pellet source.

Neglecting for the moment a possible inward pinch, the diffusion coefficient for a constant density gradient scales directly proportional to the total particle source inside. Since the particle flux of HFS pellet injection is about 5 times larger than the neutral injection flux and about 7 times larger than the time derivative of the inventory, we conclude that the local particle diffusivity has increased by the same amount during the pellet phase with respect to the preceeding phase with beam core fueling only. Allowing for an inward pinch makes the subject more complicated but does not change the qualitative conclusion. Although this rough analysis suggests a critical gradient behaviour, much more detailed work and comparison with the best available 3D turbulence simulation codes [18,19] are necessary for better understanding.

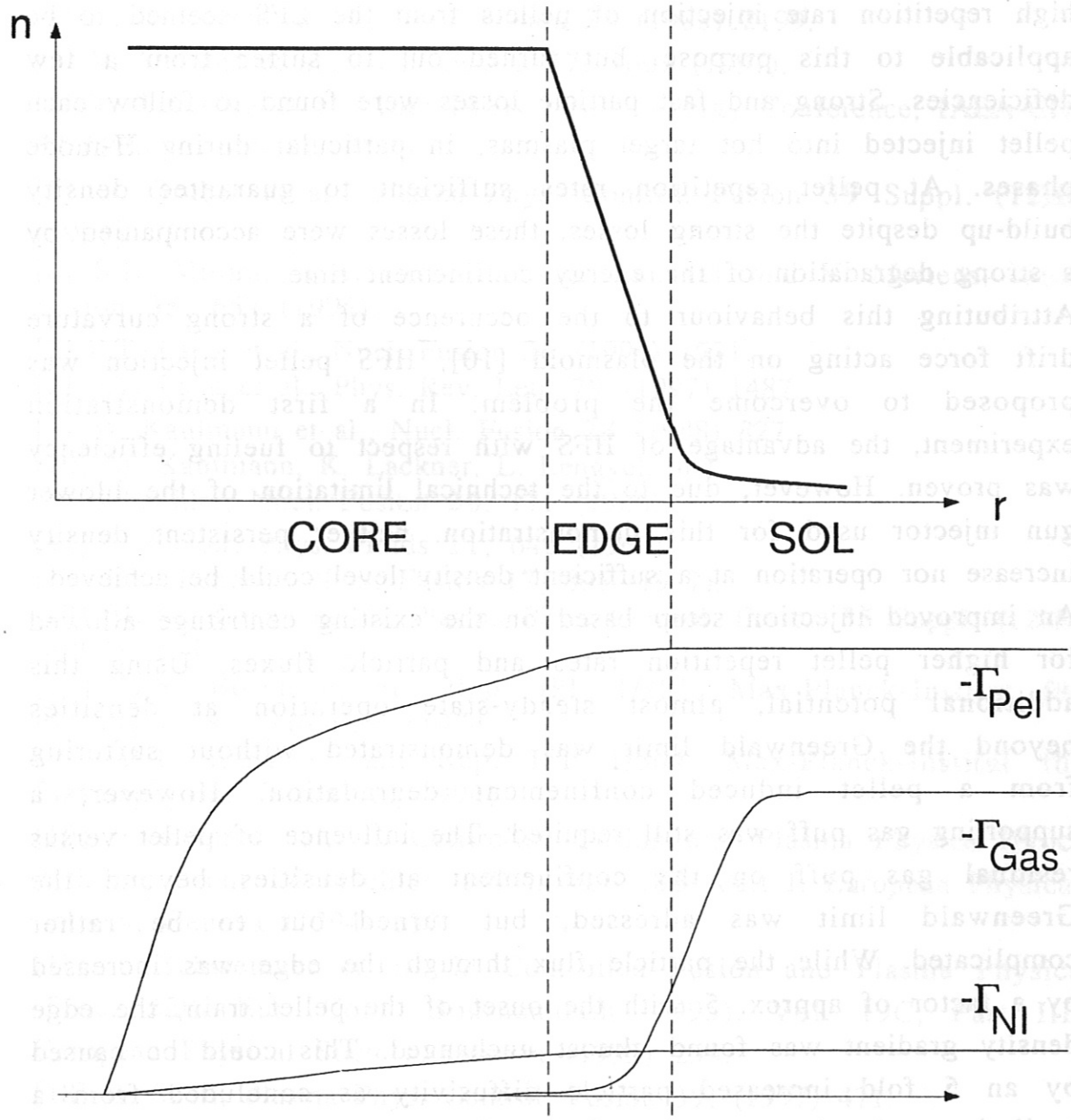

Figure 10: Schematic of different particle source contributions. Gas puff and recycling neutrals are ionized in the scape-off layer and the separatrix vicinity, while the neutral beam source and the pellet deposition are located mostly inside the edge gradient zone. In steady state, the ion outflow through the steep gradient region is about equal to the sum of the total beam and pellet particle influx.

5. SUMMARY AND CONCLUSION

Experiments were performed on ASDEX Upgrade to demonstrate the feasibility of operating a tokamak in steady-state at a density beyond the empirical Greenwald limit. During previous investigations, the high repetition rate injection of pellets from the LFS seemed to be applicable to this purpose, but turned out to suffer from a few deficiencies. Strong and fast particle losses were found to follow each pellet injected into hot target plasmas, in particular during H-mode phases. At pellet repetition rates sufficient to guarantee density build-up despite the strong losses, these losses were accompanied by a strong degradation of the energy confinement time.
Attributing this behaviour to the occurence of a strong curvature drift force acting on the plasmoid [10], HFS pellet injection was proposed to overcome the problem. In a first demonstration experiment, the advantage of HFS with respect to fueling efficiency was proven. However, due to the technical limitation of the blower gun injector used for this demonstration, neither persistent density increase nor operation at a sufficient density level could be achieved.
An improved injection setup based on the existing centrifuge allowed for higher pellet repetition rates and particle fluxes. Using this additional potential, almost steady-state operation at densities beyond the Greenwald limit was demonstrated without suffering from a pellet induced confinement degradation. However, a supporting gas puff was still required. The influence of pellet versus residual gas puff on the confinement at densities beyond the Greenwald limit was adressed, but turned out to be rather complicated. While the particle flux through the edge was increased by a factor of approx. 5 with the onset of the pellet train, the edge density gradient was found almost unchanged. This could be caused by an 5 fold increased particle diffusivity as concluded from a preliminary local tranport analysis. A much more detailed local analysis and comparison with available turbulence codes is necessary to provide deeper insight into this phenomenon.

REFERENCES

[1] R. Aymar, V. Chuyanov, M. Huguet, R. Parker, Y. Shimomura, 16th IAEA Fusion Energy Conference, IAEA-CN-64/FP-1 (Montreal, 1996).

[2] N. Greenwald et al., Nucl. Fusion **28** (1988) 2199.

[3] V. Mertens et al., Nucl. Fusion **37**, 1607 (1997).

[4] T. Takizuka et al., 16th IAEA Fusion Energy Conference, IAEA-CN-64/FP20 (Montreal, 1996).

[5] O. Gruber et al., Plasma Phys. Control. Fusion **39** Suppl. (12)B, (1997) 19.

[6] S.L. Milora, W.A. Houlberg, L.L. Lengyel, and V. Mertens, Nucl. Fusion **35**, 657 (1995).

[7] P.T. Lang et al., Nucl. Fusion **36** (1996) 1531.

[8] P.T. Lang et al., Phys. Rev. Lett. **79** (1997) 1487.

[9] M. Kaufmann et al., Nucl. Fusion **28** (1988) 827.

[10] M. Kaufmann, K. Lackner, L. Lengyel, and W. Schneider, Nucl. Fusion **26**, 171 (1986).

[11] J. Junker, Phys. Fluids **11**, 646 (1968).

[12] L.L. Lengyel, Nucl. Fusion **17**, 805 (1977).

[13] M. Kaufmann et al., Plasma Phys. Control. Fusion **35** Suppl. (12)B, (1993) 205.

[14] H.S. Bosch et al., Rep. IPP 1/281, Max-Planck-Institut für Plasmaphysik, Garching (1994).

[15] P.T. Lang et al., Rep. IPP 1/304, Max-Planck-Institut für Plasmaphysik, Garching (1996).

[16] F. Ryter et al., in Controlled Fusion and Plasma Physics (Proc. 21th Eur. Conf. Montpellier, 1994), Vol. 18B, Part I, European Physical Society, Geneva (1994) 330.

[17] J. Schweinzer et al., in Controlled Fusion and Plasma Physics (Proc. 22th Eur. Conf. Bournemouth, 1995), Vol. 19C, Part III, European Physical Society, Geneva (1995) 253.

[18] B. Scott, Plasma Phys. Control. Fusion **39**, (1997) 471.

[19] A. Zeiler et al., Phys. Plasmas **4**, (1997) 991.